Carcinogenic Potential of Metal Nanoparticles in BALB/3T3 Cell Transformation Assay

G. L. Sighinolfi,[1] E. Artoni,[2] A. M. Gatti,[3] L. Corsi[1]

[1]Life Sciences Department, University of Modena and Reggio Emilia, Modena, Italy

[2]Department of Neuroscience, Biomedical and Metabolic Sciences, University of Modena and Reggio Emilia, Modena, Italy

[3]Institute for Advanced Sciences Convergence & Int'l Clean Water Institute, Herndon, Virginia

Received 18 March 2014; revised 16 September 2014; accepted 1 October 2014

ABSTRACT: Metal-based nanoparticles (NPs), are currently used in many application fields including consumer products, pharmaceuticals, and biomedical treatments. In spite to their wide applications, an in-depth study of their potential toxic effects is still lacking. The aim of the present research was to investigate the potential initiator or promoter-like activity of different metallic NPs such as gold, iron, cobalt, and cerium using the Balb/3T3 two-stage transformation assay. The results indicated that all the selected metallic NPs, except for cobalt, when used as initiators did not induce any transformation in Balb/3T3 cell line. Moreover, Au and Fe_3O_4 NPs, when used in place of the tumor promoter treatment TPA, increased significantly the number of Foci/dish as compared to the MCA treatment alone. The number of Foci/dish was 2.6 for Au NPs and 2.13 for Fe_3O_4 ones, similar to those obtained by the positive control treatment (MCA + TPA), whereas 1.27 for MCA treatment alone. On the contrary, CeO_2 NPs did not show any difference in the number of Foci/dish, as compared to MCA alone, but it decreased the number of foci by 65% in comparison to the positive control (MCA + TPA). As expected, cobalt NPs showed an increased cytotoxicity and only a few surviving cells were found at the time of analysis showing a number of Foci/dish of 0.13. For the first time, our data clearly showed that Au and Fe_3O_4 NPs act as promoters in the two stage transformational assay, suggesting the importance to fully investigate the NPs carcinogenic potential with different models. Environ Toxicol 31: 509–519, 2016.

Keywords: cancerogenesis; nanoparticles; two-stage transformation assay; cytotoxicity; CFE

INTRODUCTION

In recent years, much attention has been paid to nanotechnology and its new wide range of potential applications. Particularly, metal-based NPs such as gold, iron, cobalt, and cerium, thanks to their variety and characteristics, are already being used in several application fields including consumer products, pharmaceuticals, and biomedical treatments (Nohynek et al., 2007, Wang et al., 2008).

Correspondence to: L. Corsi; e-mail: lorenzo.corsi@unimore.it

Published online 30 October 2014 in Wiley Online Library (wileyonlinelibrary.com). DOI: 10.1002/tox.22063

Gold NPs are already being tested as a drug delivery carrier (Chen et al., 2008, Boisselier and Astruc, 2009) to cure leukaemias and autoimmune diseases (i.e., rheumatoid arthritis, lupus erythematosus). Super-paramagnetic Iron Oxide NPs (Fe_3O_4, SPION) are being tested as enhancers of contrast in nuclear magnetic resonance imaging, as drug delivery carriers and even as a multifunctional platform for the inhibition of bacteria biofilm during the infection process (Petri-Fink and Hofmann, 2007; Ravizzini et al., 2009; Burtea et al., 2011; Durmus et al., 2013). The biomedical special interest of cerium NPs is represented by their radio protective effect in radiotherapy of cancer diseases. The unique property of cerium NPs is represented by the ability to exceed all traditional antioxidants and to exert radio

protective properties in biological media (Hirst et al., 2011; Shcherbakov et al., 2011; Wason and Zhao, 2013). Cerium NPs are now even being studied as possible neuro protectors after ischemia process (Estevez et al., 2011).

Cobalt NPs are being tested as a noninvasive method for eradicating cancer cells by using thermal therapy and radio frequency radiation (Xu et al., 2008), as components of glucose biosensors or in ophthalmic procedures (Rutnakornpituk et al., 2002). Since the constant increase of metallic NPs in biomedical applications, several studies have been already carried out to evaluate the possible cytotoxicity of these new materials. However, few studies have focused on their carcinogenic potential. The ability of NPs to stimulate target cells to produce reactive oxygen species in target cells might induce an increased genetic instability that could be associated with cancer development (Shuo et al., 2014).

Ponti et al. in 2009 showed the genotoxicity of cobalt NPs (Co NP 100–500 nm) as compared to cobalt ions (Co^{2+}). They found that Co NPs are able to induce genotoxic effects in human isolated leukocytes although their mechanisms of action are not very clear. The high variability in the genotoxic effects seems to be related to their size and internalization process and was found to be less efficient than cobalt ions one. Additional *in vitro* studies concerning the concurrent cytotoxicity and transforming capacity of Co NPs in a Balb/3T3 cell line have revealed that such NPs can gradually dissolve in culture media releasing Co^{2+} (Papies et al., 2007).

Recently, it has been shown that iron oxide NPs (Fe_3O_4-Magnetite) were able to induce a dose dependent cytotoxic effect in human skin epithelial A431 cells and in A549 lung epithelial cells. Moreover, after 24 h of exposure, NPs were able to exert genotoxic effect, as measured by the Comet assay (Ahamed et al., 2013).

These results prompted us to investigate the potential initiator or promoter-like activity of different metallic NPs such as gold, iron, cobalt, and cerium. The two-stage transformation assay mimics an initiation/promotion regimen of multistage carcinogenesis *in vivo* (Mondal et al., 1976; Boreiko, 1986) and therefore appears to be an appropriate *in vitro* assay for metallic NPs to evaluate their possible promoter-like activity.

MATERIALS AND METHODS

Nanoparticles Characterization

Four different spherical types of NPs were purchased in dust form: Au (50–100 nm), Co (28 nm), Fe_3O_4 (20–50 nm), CeO_2 (15–30 nm) NPs (Nanostructured & Amorphous Materials, Houston, TX). The NPs were depirogenated for 100 min at 190°C and suspended in phosphate buffered saline (PBS) (GIBCO Invitrogen, Karlsruhe, Germany) at pH 7.5, then sonicated in a Branson 3510 Ultrasonic bath (Branson Ultrasonics, Danbury, CT) for 20 min and filtered through a 0.2 micron filter. Strong vortexing before each test to avoid micro clusters formation and NPs aggregation was carried out. Figure 1 shows the morphology of the different NPs by means of a Field Emission Gun Environmental Scanning Electron Microscope (FEG-ESEM) (Quanta 250, FEI, The Netherlands). The observations occurred at low vacuum, from 30 to 8 keV, in secondary and backscattered mode, at 10 mm of working distance (WD). An Energy Dispersive X-ray Spectroscopy (EDS) (EDAX, USA) detector, coupled to FEG-ESEM, was used to identify the chemical composition of the NPs.

The NPs suspensions were characterized using the following techniques:

1. Zeta Potential (Z-Potential) (Malvern ZetaSizer Nano ZS, UK) operating at a light source wavelength of 532 nm and a fixed scattering angle of 173° to determine changes in the surface state and charge.
2. Dynamic light scattering (DLS) (Malvern Zetasizer Nano ZS, UK) to define the hydrodynamic diameter of the NPs dispersion.

Each solution was analyzed at 25°C, in triplicate. Hydrodynamic diameters were calculated using the internal software analysis from the DLS, intensity-weighted particle size distribution and each measurement was the average of 20 data sets acquired for 10 s each (Table I).

Cell Culture

BALB/3T3 clone A31-1-1 cells were provided by the Istituto Zooprofilattico Sperimentale (IZSBS, Brescia, Italy). The defrozen cell cultures assays were always maintained in a subconfluent state (less than 80% of confluence). Cells were cultured using Dulbecco's Modified Eagle's Medium (DMEM) supplemented with 10% FBS (Australian origin) and 0.5% (v/V) Penicilline-Streptomicine (Invitrogen, Italy). Two-stage transformation assays were performed using a mix of Eagle's minimal essential medium (EMEM), and Ham F-12 medium and ITES (5000 μg bovine pancreas insulin, 10,000 μg human transferrin, 1530 μg ethanolamine, and 4.3 μg sodium selenite in a vial) (Invitrogen, Italy). Final medium was prepared by adding an equal volume of EMEM and Ham F-12 medium with 1% ITES and 5% FBS. Cell cultures were maintained in standard conditions (95% humidity, 5% CO_2, 37°C).

CFE and XTT Assays

To assess NPs toxicity on BALB/3T3 clone A31-1-1 cells, a colony-forming efficiency (CFE) and XTT cell viability assay were performed with different NPs concentrations. For the CFE assay, cells were plated in 60 mm petri dishes with 5 mL of DMEM medium at the density of 5×10^4 cells/dish. Twenty-four-hours after seeding the cells were counted (Bürcker chamber) and treated with each type of NPs at the

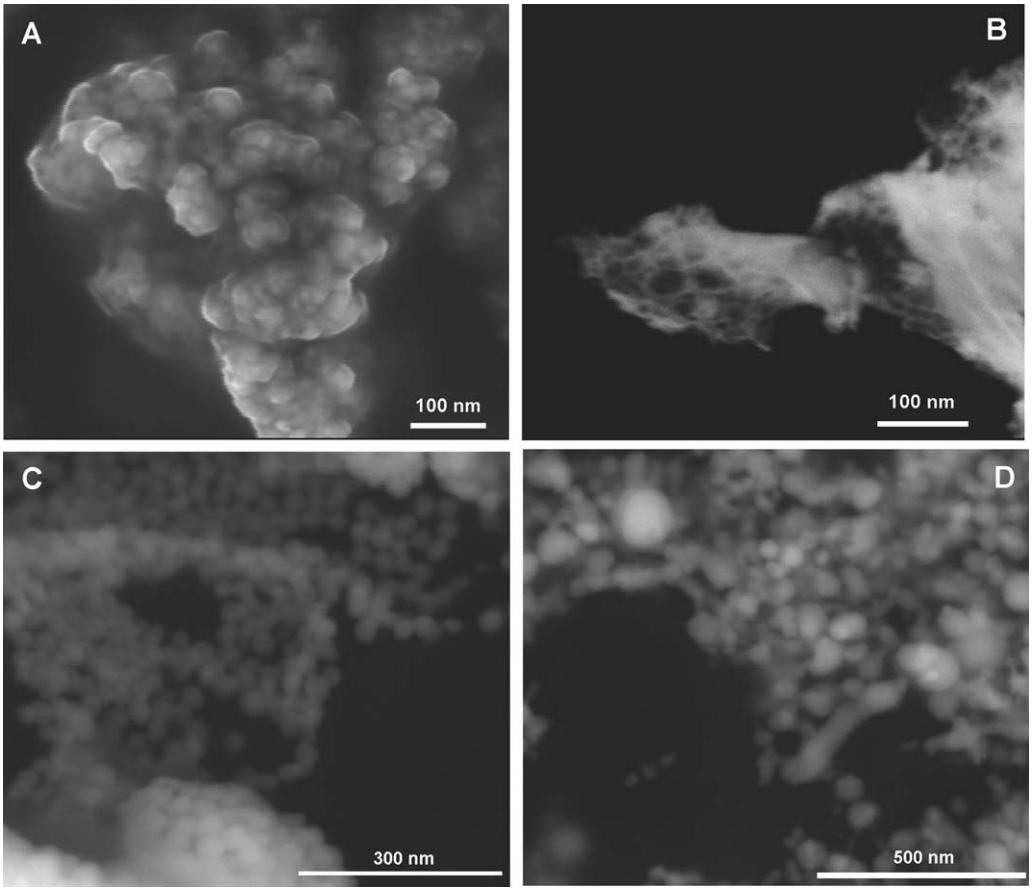

Fig. 1. FEG-ESEM images of suspended NPs. (A) Fe_3O_4, (B) CeO_2, (C) Au, and (D) Co.

concentrations of 1, 10, 50, and 100 μ*M* that corresponds to 0.2, 2, 10, 20 μg/mL, respectively. NPs concentrations in the growth media were obtained by adding a given amount of particles to the medium. Cells plated in petri dishes without NPs were the negative control, while cell exposed to 0.125% (w/v) phenol (Sigma Aldrich, St Louis, MO), were the positive control. The viability of the cells was preliminarily assessed by observing the degree of their adhesion to the substratum and their morphology after 24 h of incubation time with the NPs. Then, the cells were stained with Giemsa (Sigma-Aldrich, St. Louis, MO) for the microscopic evaluation (Optical microscope, Nikon TMS, Japan). After 48 and 72 h, the total number of cells was counted and the ability to form colonies (groups of at least 16 cells) was assessed.

For XTT assay, cells were plated in 96 wells microplates (NUNC, USA) at a concentration of 7×10^3 cells/well in a volume of 100 μL of medium. After 3 h of incubation time the cells were treated using the four types of metallic NPs at different concentrations (1, 10, 50, and 100 μ*M*). After 48 or 72 h of NPs contact, 50 μL of XTT labeling mixture solution was added to each well. After 8 h the plates were analyzed using a spectrophotometer (Multiskan RC, ThermoLabsystems™, Finland) at a wavelength of 492 nm. Nontreated cells were used as negative control, while cells treated with PBS acted as solvent control and cells treated using 0.125% (w/v) phenol served as positive control. Results were expressed as an average of five independent experiments. NPs spectrophotometrical interference was estimated performing preliminary readings with NPs and PBS.

Two-Stage Cell Transformation Assay

The two-stage cell-transformation assay is based on BALB/c 3T3 cells treatment with a sub-threshold dose of a tumor initiator 3-methylcholanthrene (MCA) at the beginning of

TABLE I. Mean size distribution (nm) ± SD of NPs after PBS suspension at different time points

	Average Diameter (nm) in PBS			
NPs	24 h	48 h	72 h	PDI
Au	190 ± 10.1	187 ± 20.1	180 ± 28.6	1
Co	122 ± 11.3	141 ± 11.2	134 ± 12.4	0.81
Fe_3O_4	161 ± 12.4	159 ± 15.7	178 ± 11.7	0.77
CeO_2	171 ± 23.1	175 ± 19.8	188 ± 17.3	0.89

Poly Dispersivity Index (PDI) value has been included.

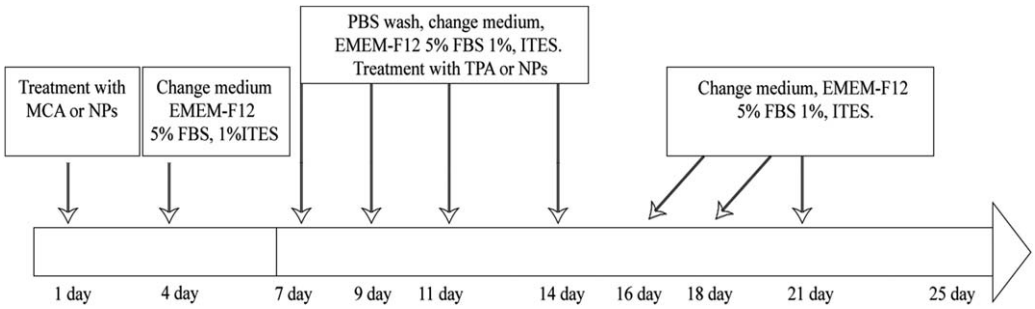

Fig. 2. Scheme of two-stage transformation assay. Initiation phase, day 1–7. On day 1, subconfluent Balb/3T3 cell culture was treated with MCA 0.5 μg/mL (positive initiator) or metal NPs (10 μ*M* of $Fe_3O_4/CeO_2/Au/Co$ NPs) as initiator stimuli and reseeded in DMEM medium supplemented with 10% FBS. On day 4 medium was changed. Promotion started on day 7 and ended on day 25. In promotion phase, cells were cultured in DMEM medium supplemented with 5% FBS and 1% ITES. On days 7, 11, and 14 cells were treated with TPA 300 ng/mL (positive promoter) or metal NPs (2.5 μ*M* of $Fe_3O_4/CeO_2/Au/Co$ NPs) as promoter stimuli to reach the final 10 μ*M* dilution. After two weeks cells were normally seeded with ITES medium for another four weeks.

cultivation and then with a tumor promoter 12-O-Tetradecanoylphorbol 13-acetate (TPA) to induce preneoplastic foci. This type of two stage cell transformation (initiation and promotion) assay *in vitro* is similar to two-stage carcinogenesis *in vivo* tests (Kuroki and Sasaki, 1985; Sakai and Fujiki, 1991). The two stage transformation assay used to test the NPs was based on the improved method proposed by Kajiwara et al., 1997. In particular, it was used a special medium supplemented with a mixture of insulin, transferrin, ethanolamine, and sodium selenite (ITES) and a low concentration of fetal bovine serum (FBS). It was demonstrated that this medium together with MCA+TPA treatment caused high frequency transformation with foci appearing after 45 days instead of the 90 days required by the original protocol. NPs were tested in various combinations as potential initiators, promoters or both: NPs at the concentration of 10 μ*M* were used with/without MCA or TPA following the two-stage protocol (Fig. 2).

Actively growing cells were seeded at a density of 5×10^4 cells/dish in 5 mL of DMEM culture medium. Twenty-four-hours after seeding the cells were treated with/without the tumor initiator MCA at the concentration of 0.5 μgr/mL with/without NPs. After three days the medium was changed and ITES cell medium was added for another three days. Cells were then treated with/without the tumor promoter TPA at the concentration of 300 ngr/ml with/without NPs, for two weeks. After two weeks cells were normally seeded with ITES medium for another four weeks. After foci formation cells were fixed with 100% methanol and stained with a 2 mL of GIEMSA 1:10 solution. Tumor foci were manually scored for morphological transformation under stereomicroscope as described by the International Agency for Cancer Research (IARC) Working Group (IARC/NCI/EPA, 1985). To evaluate culture conditions, plating efficiency (PE, calculated as the mean of colonies in CFE/dish × 100) and Survived cells (SC, calculated as the total number of cells × PE/100) were estimated.

Electron Microscopy Analysis

The NPs uptake by cells was investigated by means of Scanning and Transmission Electron Microscopy (STEM and TEM). For the TEM (Jeol 1200' EXII, Japan) observations, ultra-thin sections (70-nm thick) were cut with an ultracut microtome (Ultracut Reichert, USA), collected on 150-mesh copper grids and stained with uranyl acetate and lead citrate. TEM observations were performed using EDS analyses (Inca 100, Oxford) to check the NPs chemical composition.

For STEM observations (FEG-ESEM Quanta 250, FEI Company, the Netherlands), cells were cultured at a density of 5×10^5 in a 75 cm^2 flask (Corning Incorporated, NY) with 20 mL of complete culture medium. Cells were exposed to NPs at the concentration of 10 μ*M* for 48/72 h. After exposure, the medium was removed and cells were washed with PBS and then detached from the substrate using trypsin (Sigma–Aldrich, Italy) and centrifugated at 1000 rpm for 5 min. The cell pellets were thoroughly washed with PBS buffer and fixed in a solution of 2.5% (v/v) (Sigma–Aldrich, Italy) for 90 min at 4°C. They were then rinsed with PBS and postfixed in 1% (v/v) osmium tetroxide aqueous solution (Sigma–Aldrich, Italy) for 1 h. Cells were later dehydrated in an ascending graded series of ethanol (30, 60, 70, 90, and 100%, v/v), and embedded in epoxy resin (FlukaBioChemika, Switzerland). The resin was polymerized at 60°C for 48 h. The ultra-thin sections (60–70 nm) obtained with an ultracut microtome (Ultracut Reichert, USA) mounted on a copper grid were analyzed under the FEG-ESEM microscope.

The same microscope was used to analyze the Type III foci obtained after treatments in the two-stage transformation assay. Cells were cultured in 60 mm petri dishes in which a 13-mm diameter plastic coverslip (Thermanox Plastic Coverslips, NUNC, USA) was placed, with 5 mL of DMEM medium at the density of 5×10^4 cells/dish. Cells were treated with/without NPs at the dilution of 10 μ*M* for

48/72 h with/without MCA or TPA as described in two-stage transformation assay. Thereafter, treated and untreated (control) cells were extensively washed with PBS buffer, fixed in a 4% glutaraldehyde (solution Sigma-Aldrich, Italy) for 1 h and dehydrated in ascending concentration solutions of ethanol (70, 90, and 100%) for 10 min. The cells were then observed in low vacuum modality in order to preserve cells samples without further treatments or manipulations.

Statistical Analyses

In cytotoxicity assays, the total colonies data after NPs treatment were statistically analyzed as mean of three independent experiments (5 replicates each) with standard deviation and expressed as CFE% respect the negative control. Data were analyzed using one-way ANOVA model with Dunnett's comparative test. Two-stage cell transformation assay was performed in three independent experiments (5 replicates each). Experimental data were analyzed by one-way ANOVA with Bonferroni's multiple comparison test. GraphPad Prism 5 software was used to elaborate graphs and data. *P*-values of <0.05 were considered as the limit of statistical significance.

RESULTS

NPs Suspension Analysis

The NPs characterization was performed using a combination of STEM, TEM, DLS, and Zeta-potential techniques. The size distribution of NPs after PBS suspension was verified with DLS techniques at different time points. Results show that NPs once suspended form larger aggregates with diameters ranging from 122 ± 15.1 nm (Co) to 190 ± 10.1 (Au) nm. NPs suspensions remain rather stable after 48 and 72 h (Table I). The presence of a single peak in the size distribution confirmed that NPs were monodispersed. TEM results of gold, cobalt, iron oxide, and cerium oxide NPs confirmed the NPs tendency to aggregate and to form clusters. *Z*-potential measurements of the suspensions indicated values of: -10 mV for Au NPs, -8.2 mV for Co NPs, -10.6 mV for Fe_3O_4 NPs, and $-8{,}4$ mV for CeO_2 NPs.

Cytotoxicity

The NPs cytotoxicity was evaluated on Balb/3T3 cell by colony forming efficiency (CFE) assay and by XTT assay. Cells were exposed to NPs at concentrations ranging from 1 to 100 μM and at the exposure times of 48 and 72 h. We focused our attention on 72 h exposure time, since no significant difference in cytotoxicity was detected between the two times of exposure (data not shown). The results obtained by CFE assay (Fig. 3) showed toxicity for all types of NPs at the 50 μM concentration. Cobalt NPs showed greater toxicity by decreasing the number of colonies from 32% to 48% even at lowest dilutions (1 and 10 μM) as compared to the negative control. At the concentration of 1 or 10 μM Au, Fe_3O_4 and CeO_2 NPs did not exert significant cytotoxicity on Balb/3T3 at all times tested. Using XTT assay on Balb/3T3 to evaluate cell viability at the same concentrations and exposure times, we observed that Au, Fe_3O_4, and CeO_2 NPs were able to decrease significantly the cell viability by over 18% only at 100 μM concentration. Cobalt NPs on the contrary showed a reduction of nearly 98%, so affecting the cell viability even at the lowest concentration tested (1 μM) (Fig. 3).

NPs Carcinogenic Potential

To evaluate the NPs carcinogenicity, the two-stage cell transformation was selected using the 10 μM NPs concentration on the base of the toxicological results of the CFE and XTT assays. In fact, 10 μM is the maximum concentration of NPs, which did not show cytotoxic effects (except for Co NPs) and, at the same time, possessed the best PDI (Poly Dispersivity Index).

The NPs as initiators alone or in combination with TPA (NPs + TPA), did not produce tumor foci except in the case of cobalt which, in spite of its toxicity found in XTT and CFE assays, confirmed a carcinogenic effect on the Balb/3T3 cells, acting as initiator (Co alone and Co + TPA). The incubation of Balb/3T3 cells with Co NPs alone produced a number of Foci/dish of 0.2 (Table II). The ability to decrease cell viability and proliferation did not prevent foci formation after only three days (72 h) of exposure with a number of Foci/dish of 1.8 (Table II). Surprising results were obtained using the NPs in place of the tumor promoter treatment TPA (MCA + NPs). In particular Au and Fe_3O_4 NPs increased significantly the number of Foci/dish compared to the MCA treatment alone ($^*P < 0.05$). The number of Foci/dish was 2.6 for Au NPs and 2.13 for Fe_3O_4, similar to those obtained by the positive control treatment (MCA + TPA), whereas 1.27 for MCA treatment alone.

Different results were obtained using cerium oxide NPs. Indeed, the data did not show any difference in the number of Foci/dish, between the CeO_2 NPs administered as tumor promoter and the MCA alone (Table II). In addition, CeO_2 NPs treatment showed a dramatic and significant decrease in the number of foci (-65%,$^{***}P < 0.001$), when compared to the positive control (MCA + TPA) as reported in Table II.

As expected, cobalt NPs showed an increased toxic effect due to the prolonged time of exposure (>96 h). In fact, at the end of the treatment, only a few surviving cells were found upon contact (CFE = 51%) showing a number of Foci/dish of 0.13 with a significant decrease versus MCA and versus the positive control MCA + TPA ($^*P < 0.05$).

Predominantly Type III foci were found after NPs treatments. Type III foci are dense, multilayered, and basophilic, with a random orientation of cells at the focus edge and invasion into the monolayer (Fig. 4).

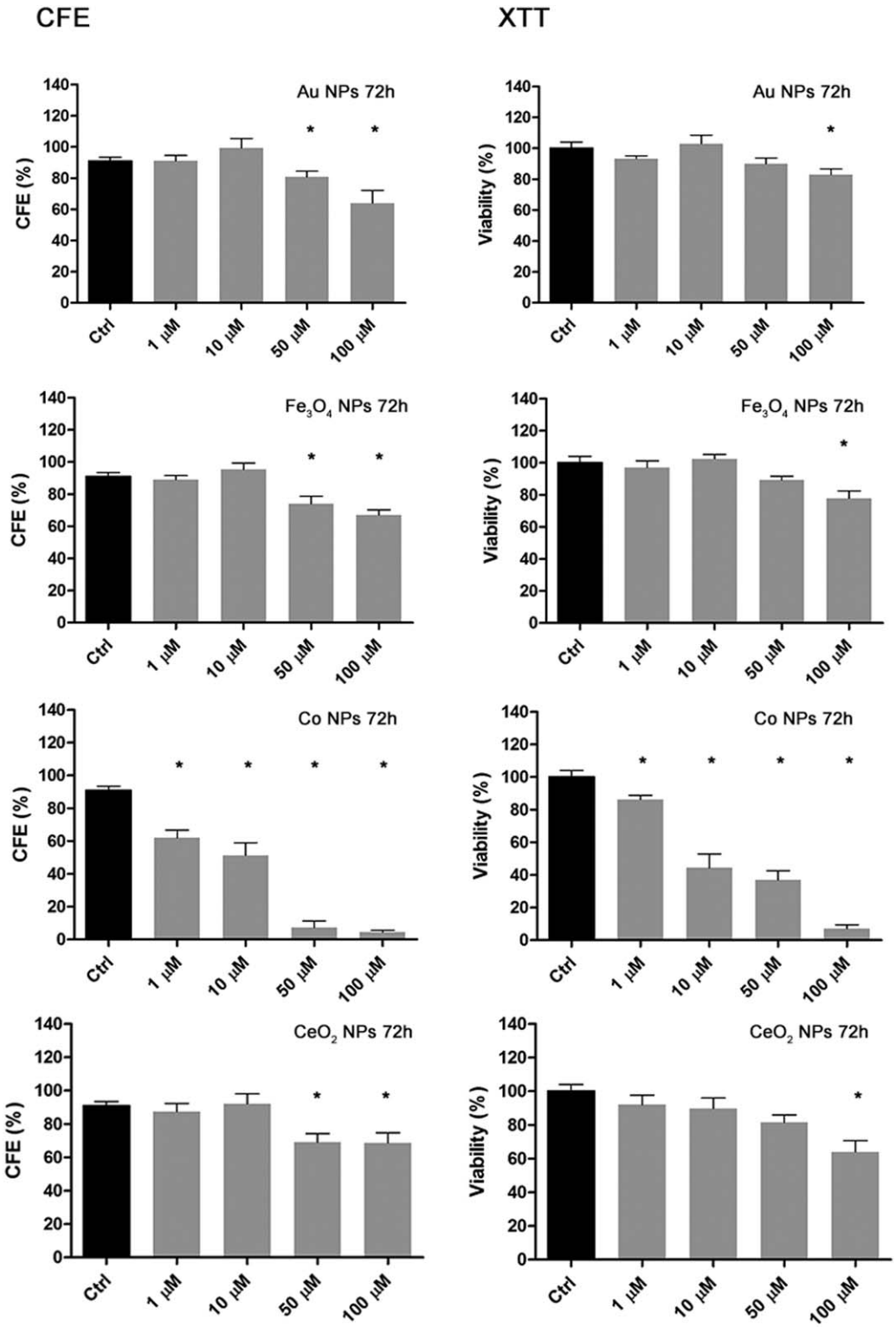

Fig. 3. Cytotoxicity of NPs (gray histogram) versus negative control (black histogram). Colony forming efficiency (CFE) of Balb/3T3 cells exposed for 48 and 72 h to increasing concentration of NPs (1–100 μM). All NPs except cobalt NPs induced cytotoxicity in Balb/3T3 cells at 72 h of exposure at concentration >10 μM. Cobalt NPs were the only particles exerting a toxic effect even at the 1 μM concentration. Data, mean of three independent experiments (three replicates each) $\pm$ standard deviation (SD), were analyzed in comparison to the solvent control and evaluated by one-way ANOVA and Dunnet post test ($^*P < 0.05$). XTT cell viability test on Balb/3T3 cells exposed 48 and 72 h confirmed nearly the same results thus showing decreased cell viability for all NPs except cobalt only at the 100 μM highest concentration. Data, mean of three independent experiments (three replicates each) $\pm$ standard deviation (SD) were analyzed in comparison to the negative control and evaluated by one-way ANOVA and Dunnet post-test ($^*P < 0.05$).

TABLE II. Two-stage transformation assay results after Au, Co, Fe_3O_4, CeO_2 NPs exposure

	CFE%	PE %	Survived Cells	No. of Foci	Foci/dish	No. of Dishes Examined
NEG	100	33.33	166,666	0	0	15
MCA	31	10.33	51,666	19	1.27	15
TPA	49	16.33	81,666	0	0	15
MCA+TPA	81	27	135,000	38	2.53	15
Au	99	33	165,000	0	0	15
Fe_3O_4	95	31,66667	158333.3	0	0	15
CeO_2	92	30,66667	153333.3	0	0	15
Co	62	20,66667	103333.3	3	0.2	15
MCA+Au	93	31	155,000	39	2.6	15
MCA+Fe_3O_4	82	27.33	136,666	32	2.13	15
MCA+CeO_2	92	30.66	153,333	17	1.13	15
MCA+Co	51	17	85,000	2	0.13	15
Au+TPA	70	23.33	116,666	0	0	15
Fe_3O_4+TPA	82	27.33	136,666	0	0	15
CeO_2+TPA	85	28.33	141,666	0	0	15
Co+TPA	51	17	85,000	27	1.8	15

Nanoparticles Cell Interaction

STEM observations clearly showed a general NPs cellular internalization. At morphological level, cells looked healthy, proliferating and well preserved. No evidence of cytoskeleton structure changes, cell sufferance, or apoptosis was found. NPs were found within phagocytic vacuoles or spread in the cytoplasm. Iron oxide and gold NPs were also found in close contact to the nuclear area of Balb/3T3 cells as shown in Figure 5. The Type III foci ESEM observation revealed a dense, multilayered morphology. In addition, the ESEM images clearly showed the cell foci invasion into the monolayer (Fig. 6). In all the images the presence of all types of NPs in clustered form was found mostly coincident to the cell foci.

DISCUSSION

In recent years the use of metallic NPs has been widely used in many different fields, such as the medical-pharmaceutical industry. Several studies of nanomedicine have shown the

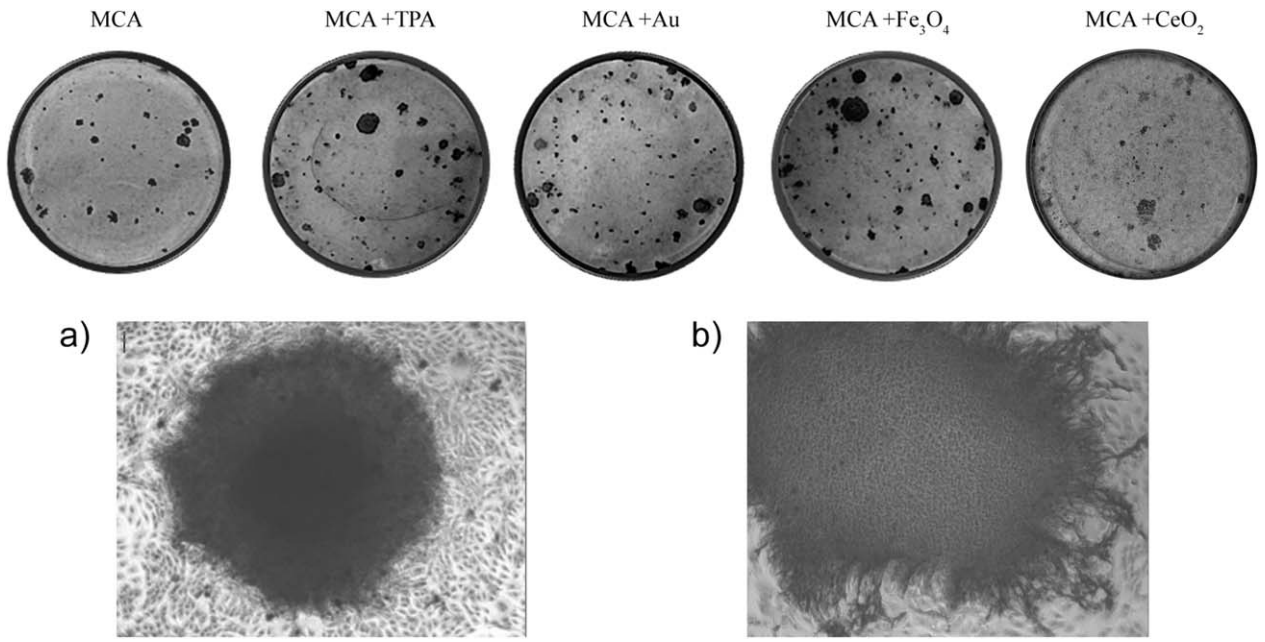

Fig. 4. Foci formation in Balb/3T3 cells after MCA, MCA + TPA, and MCA + NPs treatments. Optical images (×40) of type III foci after (A) Au NPs treatment or (B) Fe_3O_4 NPs treatment.

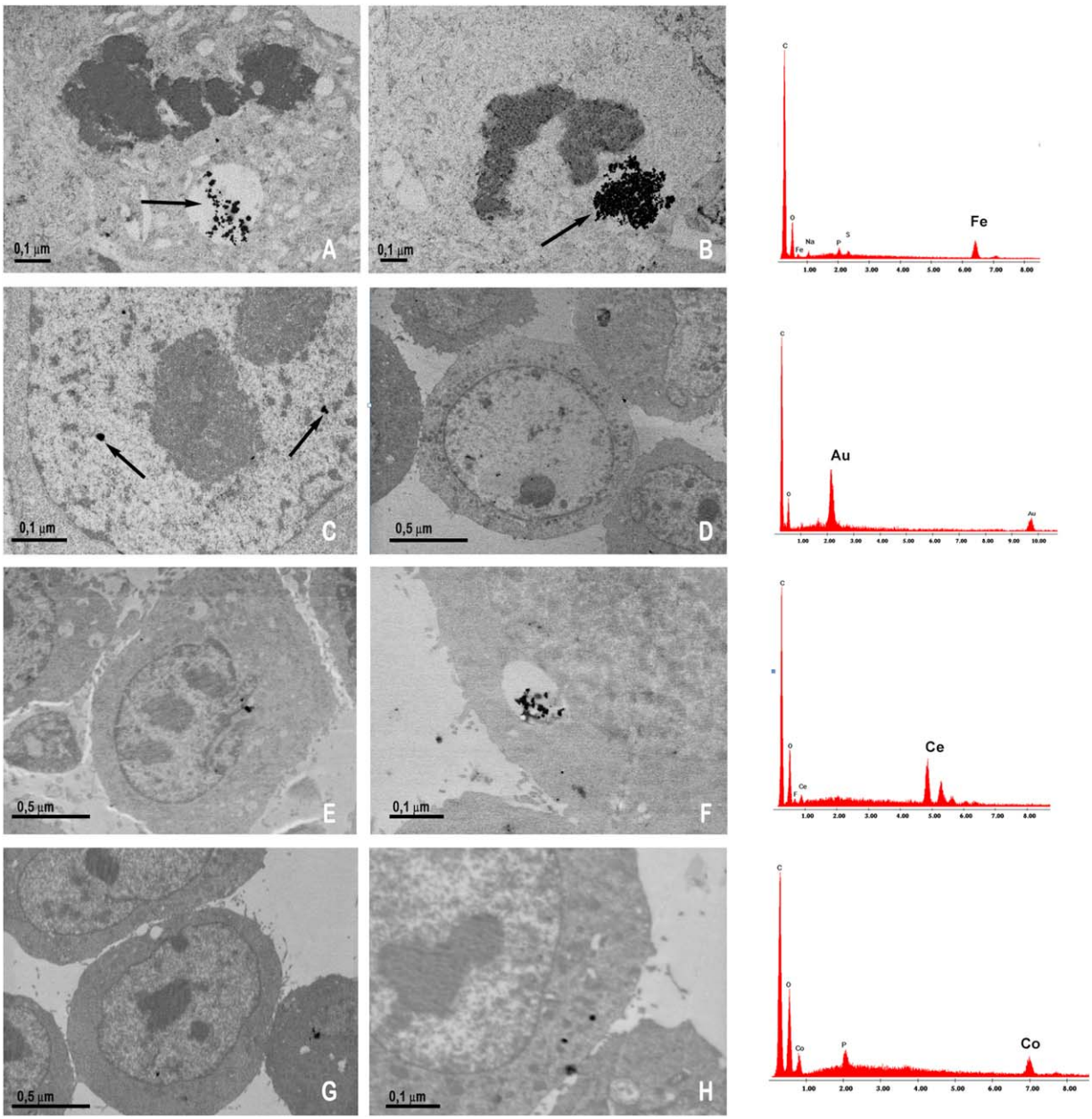

Fig. 5. TEM (A, B, C, D) and STEM images (E, F, G, H) of NPs inside the Balb/3T3 cells. Image (A) presence of Fe_3O_4 nanoparticles inside vacuoles in the nuclear area of a mitotic cell. Image (B) Fe_3O_4 nanoparticles in the nuclear area of a mitotic cell. Image (C) nonmitotic cell nucleus with two Au particles micro-clusters. Image (D) Au nanoparticles internalized by the cells. Images (E, F) CeO_2 NPs inside the cell cytoplasm or entrapped into vesicles. Image (H) Co NPs in close contact with the cell membrane. Image (G) Co NPs inside the cell membrane. On the right side of each panel the EDS spectrum of the NPs is reported. [Color figure can be viewed in the online issue, which is available at wileyonlinelibrary.com.]

beneficial effects of certain types of NPs for the treatment of tumors (Wang et al., 2008; Martin et al., 2013), for a selective transport of the drug to the site of action (Chen et al., 2008), and to improve the Nuclear Magnetic Resonance (NMR) imaging (Duguet et al., 2006). However, only recently, clinical studies have been performed verifying the metallic NPs potential toxicity. It has been demonstrated an enhancement of the inflammatory response by NPs in lung tissues (Zhang et al., 2012; Fariss et al., 2013) and in the central nervous system (Peters et al., 2006; Block and Calderón-Garcidueñas, 2009).

So in order to fulfill the mandatory requirement of ensuring the safety of workers, patients and the consumers/users, toxicological research with several approaches is fundamental. In this context, recently, it was shown the carcinogenic potential of cobalt NPs on cells of murine fibroblasts

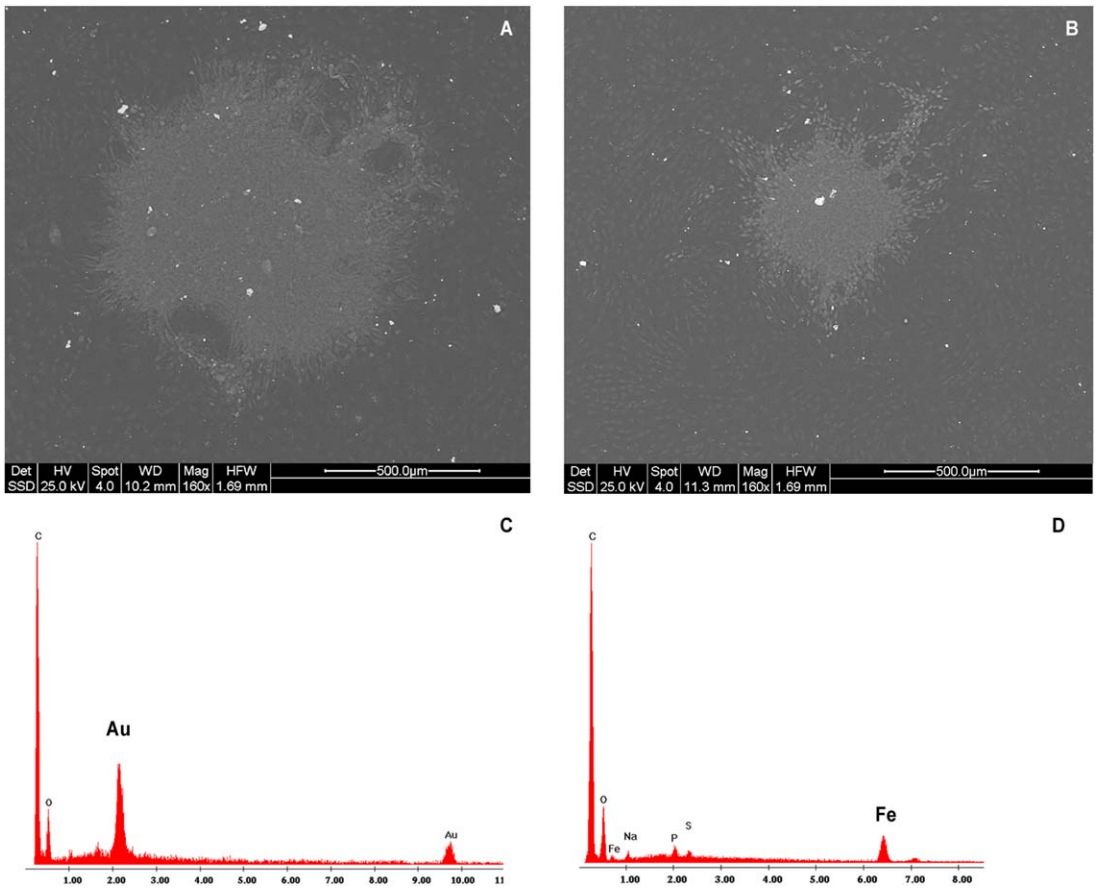

Fig. 6. ESEM images of type III foci after Au-NPs (A) and Fe_3O_4 NPs (B) treatment as promoter. EDS spectrum (C, D) of the NPs is reported. [Color figure can be viewed in the online issue, which is available at wileyonlinelibrary.com.]

(Balb/3T3) (Ponti et al., 2009). The authors clearly demonstrate that, in spite of a common toxicity test elicited by Co NPs and Co^{2+}, only Co NPs were able to induce morphological transformation and genotoxicity, suggesting that the toxic mechanisms were mostly triggered by Co NPs. These findings induced us to evaluate if different NPs were able to induce cancerogenesis using the two-stage transformational assay.

We focused our attention on Fe_3O_4, CeO_2, and Au NPs, for their medical applications as contrast agent in NMR, or as catalyst and UV adsorbent and tumor hyperthermia agents.

Co NPs at a 10 μM concentration were selected as reference cancerogenic compound to perform the two-stage transformational assay; concentration that was able to induce tumoral foci in Balb/3T3 cells (Ponti et al., 2009).

Really interestingly was the result obtained on the ability of the selected metal nanoparticles (NPs), to generate and/or promote tumoral foci in Balb/3T3 cell line. NPs showed different results depending to the respective chemical-physical properties. Indeed, while Fe_3O_4, Au, and CeO_2 NPs, when used as tumor initiators, did not give rise to any kind of neoplastic transformation, Co NPs was able to induce foci formation, confirming the data by Ponti at al. (Ponti et al., 2009).

However, the Fe_3O_4 and Au NPs when tested as a promoters showed a dramatic increase of neoplastic foci, as compared to MCA alone, reaching values similar to those obtained by the promoter TPA. The fact that Co NPs was not able to generate foci as a promoter must be attributable to its intrinsic cytotoxic activity, which does not allow the cells to reach the end point of the two stages transformation assay. Interestingly is the finding regarding the activity of CeO_2 NPs. In fact, CeO_2 NPs did not alter the number of foci obtained by MCA alone, but they decrease significantly the formation of foci when compared to the positive control (MCA + TPA), suggesting a potential antagonism in the promotion of cell transformation. It is known that many factors are involved in NPs toxicity such as size (the tiny size allows the cell internalization and a close contact with organelles, protein, and DNA), morphology, composition, surface charge, coating, aggregation, or capacity of self- assembly, capacity of conjugation (strong or weak bonds) with other components (proteins, lipids, etc.), catalytic properties or combination with other biological components. In addition, toxicity is strongly dependent on the bio-distribution capacity

of the NPs to induce local or systemic problems, on their rate of elimination and tissue localization and, very important, on whether the materials used are biodegradable or non-biodegradable (Medina et al., 2007). Taken into account all these assumptions, it becomes difficult to identify the molecular mechanisms responsible of the Balb/3T3 transformation elicited by the selected NPs.

In this context, our results indicate that at least two main hypotheses can be formulated regarding the morphological transformation elicited by Fe_3O_4, Au NPs. The first one could be related to their intrinsic physical properties, which, in turn, could interfere with several biochemical and intracellular signaling pathways, such as genotoxic activity reported for Co NPs (Ponti et al., 2009).

The second one could be related to ions release from the NPs, which might induce cytotoxicity as in the case of Co^{2+} or inflammation and therefore promotion of cell transformation. Although the latest hypothesis must be likely true, the data available in literature on Fe_3O_4, CeO_2 and Au ions, did not show any carcinogenic activity in contrast to those one found for Co^{2+} (Lison et al., 2001; Jakupec et al., 2005; Raymond and Che, 2009; Foy and Labhasetwar, 2011).

Interestingly, in our experiments we noticed that the tumoral foci were developed mostly in conjunction with the largest agglomerates of NPs. This NPs agglomerates could be a sort of scaffold for the engraftment of foci. In this context future studies are planned in order to better understand the mechanisms of NPs effects in the promotion of neoplastic transformation of cells.

Finally, our data clearly showed, for the first time, that Au and Fe_3O_4 NPs act as promoters in the two-stage transformational assay. This important result highlighted more than ever that it is essential to investigate extensively the NPs toxicological profiles in different *in vitro* and *in vivo* models, in order to identify any potential impact of NPs on human health.

REFERENCES

Ahamed M, Alhadlaq HA, Alam J, Khan MA, Ali D, Alarafi S. 2013. Iron oxide nanoparticle-induced oxidative stress and genotoxicity in human skin epithelial and lung epithelial cell lines. Curr Pharm Des19:6681–6690.

Block ML, Calderón-Garcidueñas L. 2009. Air pollution: Mechanisms of neuroinflammation and CNS disease. Trends Neurosci 32:506–516.

Boisselier E, Astruc D. 2009. Gold nanoparticles in nanomedicine: Preparations, imaging, diagnostics, therapies and toxicity. Chem Soc Rev 38:1759–1782.

Boreiko CJ. 1986. Methodology for cell transformation assays with C3H/10T1/2 mouse embryo fibroblasts. J Tissue Cult Methods 10:165–172.

Burtea C, Laurent S, Mahieu I, Larbanoix L, Roch A, Port M, Rousseaux O, Ballet S, Murariu O, Toubeau G, Corot C, Vander Elst L, Muller RN. 2011. In vitro biomedical applications of functionalized iron oxide nanoparticles, including those not related to magnetic properties. Contrast Media Mol Imaging 6:236–250.

Chen PC, Mwakwari SC, Oyelere AK. 2008. Gold nanoparticles: From nano medicine to nanosensing. Nanotechnol Sci Appl 1: 45–66.

Duguet E, Vasseur S, Mornet S, Devoisselle JM. 2006. Magnetic nanoparticles and their applications in medicine. Nanomedicine (London) 1:157–1568. Review.

Durmus NG, Taylor EN, Kummer KM. 2013. Enhanced efficacy of superparamagnetic iron oxide nanoparticles against antibiotic-resistant biofilms in the presence of metabolites. Adv Mater 25:5706–5713.

Estevez AY, Pritchard S, Harper K, Aston JW, Lynch A, Lucky JJ, Ludington JS, Chatani P, Mosenthal WP, Leiter JC, Andreescu S, Erlichman JS. 2011. Neuroprotective mechanisms of cerium oxide nanoparticles in a mouse hippocampal brain slice model of ischemia. Free Radic Biol Med 51:1155–1163.

Fariss MW, Gilmour MI, Reilly CA, Liedtke W, Ghio AJ. 2013. Emerging mechanistic targets in lung injury induced by combustion-generated particles. Toxicol Sci 132:253–267.

Hirst SM, Karakoti A, Singh S, Self W, Tyler R, Seal S, Reilly CM. 2011. Bio-distribution and in vivo antioxidant effects of cerium oxide nanoparticles in mice. Environ Toxicol 28:107–118.

IARC/NCI/EPA Working-Group. 1985. Cellular and molecular mechanisms of cell transformation and standardization of transformation assays of established cell lines for the prediction of carcinogenic chemicals: Overview and recommended protocols. Cancer Res 45:2395–2399.

Jakupec MA, Unfried P, Keppler BK. 2005. Pharmacological properties of cerium compunds. Rev Physiol Biochem Pharmacol 153:101–111.

Kajiwara Y, Ajimi S, Hosokawa A, Maekawa K. 1997. Improvement of carcinogen detection in the BALB/3T3 cell transformation assay by using a rich basal medium supplemented with low concentration of serum and some growth factors. Mutat Res 393:81–90.

Kuroki T, Sasaki K. 1985. Relationship between in-vitro cell transformation and in vivo carcinogenesis based on available data on the effects of chemicals. IARC Sci Publ 67:93–118.

Lison D, De Boeck M, Verougstraete V, Kirsch-Volders M. 2001. Update on the genotoxicity and carcinogenicity of cobalt compounds. Occup Environ Med 58:619–625.

Martin DT, Hoimes CJ, Kaimakliotis HZ, Cheng CJ, Zhang K, Liu J, Wheeler MA, Kelly WK, Tew GN, Saltzman WM, Weiss RM. 2013.Nanoparticles for urothelium penetration and delivery of the histone deacetylase inhibitor belinostat for treatment of bladder cancer. Nanomedicine 9:1124–1134.

Medina C, Santos-Martinez MJ, Radomski A, Corrigan OI, Radomski MW. 2007. Nanoparticles: Pharmacological and toxicological significance. Br J Pharmacol 150:552–558.

Mondal S, Brankow DW, Heidelberger C. 1976. Two-stage chemical oncogenesis in cultures of C3H/10T1/2 cells. Cancer Res 36(7 Part 1):2254–2260.

Nohynek GJ, Lademann J, Ribaud C, Roberts MS. 2007. Grey goo on the skin? Nanotechnology, cosmetic and sunscreen safety. Crit Rev Toxicol 37:251–277.

Papis E, Gornati R, Prati M, Ponti J, Sabbioni E, Bernardini G. 2007. Gene expression in nanotoxicology research: Analysis by differential display in BALB3T3 fibroblasts exposed to cobalt particles and ions. Toxicol Lett 170:185–192.

Peters A, Veronesi B, Calderón-Garcidueñas L, Gehr P, Chen LC, Geiser M, Reed W, Rothen-Rutishauser B, Schürch S, Schulz H. 2006. Translocation and potential neurological effects of fine and ultrafine particles a critical update. Part. Fibre Toxicol 3:13.

Petri-Fink A, Hofmann H. 2007. Superparamagnetic iron oxide nanoparticles (SPIONs): From synthesis to in vivo studies—A summary of the synthesis, characterization, in vitro, and in vivo investigations of SPIONs with particular focus on surface and colloidal properties. IEEE Trans Nanobiosci 6:289–297.

Ponti J, Sabbioni E, Munaro B, Broggi F, Marmorato P, Franchini F, Colognato R, Rossi F. 2009. Genotoxicity and morphological transformation induced by cobalt nanoparticles and cobalt chloride: An in vitro study in Balb/3T3 mouse fibroblasts. Mutagenesis 24:439–445.

Ravizzini G, Turkbey B, Barrett T, Kobayashi H, Choyke PL. 2009. Nanoparticles in sentinel lymph node mapping. Wiley Interdiscip Rev Nanomed Nanobiotechnol 1:610–623.

Raymond W-YS, Che C-M. 2009. The anti-cancer properties of gold(III) compounds with dianionic porphyrin and tetradentate ligands. Coordination Chemistry Reviews Volume 253, Issues 11–12, June, Pages 1682–1691.

Rutnakornpituk M, Baranauskas VV, Riffle JS, Connolly J, St Pierre TG, Dailey JP. 2002. Polysiloxane fluid dispersions of cobalt nanoparticles in silica spheres for use in ophthalmic applications. Eur Cells Mater 3:102–105.

Sakai A, Fujiki H. 1991. Promotion of BALB/3T3 cell transformation by the okadaic acid class of tumor promoters, okadaic acid and dinophysistoxin-1. Jpn J Cancer Res 82:518–523.

Shcherbakov AB, Ivanov VK, Zholobak NM, Ivanova OS, Krysanov EIu, Baranchikov AE, Spivak NIa, Tret'iakov IuD. 2011. Nanocrystalline ceria based materials—Perspectives for biomedical application. Biofizika 56:995–1015.

Shuo Y, Fang Z, Fang Q, Wenjun D. 2014. Water-insoluble fraction of airborne particulate matter (PM10) induces oxidative stress in human lung epithelial A549 cells. Environ Toxicol 29: 226–233.

Foy SP, Labhasetwar V. 2011. Oh the irony: Iron as a cancer cause or cure? Biomaterials 32:9155–9158.

Wang J, Wheeler D, Zhang JZ, Achilefu S, Kang KA. 2013. NIR fluorophore-hollow gold nanosphere complex for cancer enzyme-triggered detection and hyperthermia. Adv Exp Med Biol 765:323–328.

Wang X, Yang L, Chen Z, Dong M. 2008. Application of nanotechnology in cancer therapy and imaging. CA Cancer J Clin 58:97–110.

Wason MS, Zhao J. 2013. Cerium oxide nanoparticles: Potential applications for cancer and other diseases. Am J Transl Res 5: 126–131.

Xu Y, Mahmood M, Li Z, Dervishi E, Trigwell S, Zharov VP, Ali N, Saini V, Biris AR, Lupu D, Boldor D, Biris AS. 2008. Cobalt nanoparticles coated with graphitic shells as localized radio frequency absorbers for cancer therapy. Nanotechnology 19:435102.

Zhang T, Qian L, Tang M, Xue Y, Kong L, Zhang S, Pu Y. 2012. Evaluation on cytotoxicity and genotoxicity of the L-glutamic acid coated iron oxide nanoparticles. J Nanosci Nanotechnol 12:2866–2873.